Nanoscale orbital excitations and the infrared spectrum of a molecular Mott insulator: $A15-Cs_3C_{60}$

S. Shahab Naghavi,[1] Michele Fabrizio,[2] Tao Qin,[2, 3] and Erio Tosatti[2, 4]

[1]*Department of Materials Science and Engineering, Northwestern University, Evanston, Illinois 60208, USA*
[2]*International School for Advanced Studies (SISSA), and CNR-IOM Democritos National Simulation Center, Via Bonomea 265, I-34136 Trieste, Italy*
[3]*Institut für Theoretische Physik, Goethe-Universitt, 60438 Frankfurt am Main, Germany*
[4]*International Centre for Theoretical Physics (ICTP), Strada Costiera 11, I-34151 Trieste, Italy*

The quantum physics of ions and electrons behind low-energy spectra of strongly correlated *molecular* conductors, superconductors and Mott insulators is poorly known, yet fascinating especially in orbitally degenerate cases. The fulleride insulator Cs_3C_{60} (A15), one such system, exhibits infrared (IR) spectra with low temperature peak features and splittings suggestive of static Jahn-Teller distortions with breakdown of orbital symmetry in the molecular site. That is puzzling, for there is no detectable static distortion, and because the features and splittings disappear upon modest heating, which they should not. Taking advantage of the Mott-induced collapse of electronic wavefunctions from lattice-extended to nanoscale localized inside a caged molecular site, we show that unbroken spin and orbital symmetry of the ion multiplets explains the IR spectrum without adjustable parameters. This demonstrates the importance of a fully quantum treatment of nuclear positions and orbital momenta in the Mott insulator sites, dynamically but not statically distorted. The observed demise of these features with temperature is explained by the thermal population of a multiplet term whose nuclear positions are essentially undistorted, but whose energy is very low-lying. That term is in facts a scaled-down orbital excitation analogous to that of other Mott insulators, with the same spin $1/2$ as the ground state, but with a larger orbital moment of two instead of one.

I. INTRODUCTION

Crucial in atomic and molecular physics, orbital degrees of freedom are generally quenched by crystal fields and by large electron hopping rates of uncorrelated solids, where they are seldom relevant to the electronic and vibrational structure. That is no longer the case in Mott insulators, where the electrons are localized by repulsive correlations, and their wavefunctions revert from band states back to effectively atomic or molecular states, whose electronic, orbital, spin, and nuclear degrees of freedom are generally entangled in the crystalline environment. The role of orbital degrees of freedom in particular, long appreciated in transition metal compounds [1–7] is less explored in *molecular* Mott insulators (MMIs), where site symmetry is often low, and where a variety of intra-molecular interactions interfere. A fresh case study is highly desirable in these systems, particularly in connection with possible spectroscopic manifestations of orbital variables and orbital excitations. Especially appealing are MMIs where a high symmetry of the molecular site and the resulting orbital degeneracies, quenched in the uncorrelated band state but unquenched in the Mott state, demands an explicitly joint role for the spin and orbital degrees of freedom of both electrons and ions. Particularly appealing is the opportunity, typical of Mott insulators and generally only exploited by DMFT approaches, to access the main physical phenomena through theories and calculation restricted to a nanoscale size molecular site, endowed with the site's full orbital symmetry, but

with a reduced scale intra-site molecular interactions as compared to well studied atomic cases. Besides others, one major difference between them is that the nanoscale size of the molecular site shrinks the Hund's rule exchange energy J_H one to two orders of magnitude below the 1–2 eV scale typical of an atomic Mott insulator such as Sr_2CuO_3.[3] This in turn causes the intra-site electronic multiplets including orbital excitations to drop and become entangled with the lower energy nuclear vibrations, unlike e.g., transition metal compounds where the orbital excitations, way higher in energy, are purely electronic in character.[3]

The prototypical MMI compound which embodies these novel aspects is the over-expanded fulleride $A15-Cs_3C_{60}$, a $S = 1/2$ Mott insulator, where a striking superconducting state with $T_c \sim 38\,K$ also emerges under pressure from the parent insulating state.[8–14] Pressure here mostly acts by reducing the ratio U/W of the intramolecular Coulomb repulsion U over the intermolecular electron bandwidth W below a critical value of order 1–2, turning the MMI into a half-filled three-band metal state typical of other non-expanded alkali fullerides.[15] Thanks to many studies the spin structure and spin excitations of the MMI at zero pressure have been well characterized.[9,10,16–20] Their orbital counterparts are on the contrary much more obscure, making this compound an ideal laboratory for our purposes.

We focus here on the pure, dynamical MMI state, with full unbroken structural, magnetic and orbital site symmetry—a state which as in other Mott insulators,[21]

is attained in thermal equilibrium just above the antiferromagnetic Néel temperature, $T_N \sim 46\,K$ at zero pressure. In that state, A15-Cs_3C_{60} has a lattice of space group $Pm\bar{3}n$, where Mott localized electrons hop between effective C_{60}^{3-} sites of cubic symmetry, a situation qualitatively described by a high symmetry three-band Hubbard model.[22–25] In the Mott state, intersite charge fluctuations are suppressed by the large on-site Coulomb repulsion $U \gtrsim 1$ eV,[15,23] and the system can be assimilated to weakly coupled effective molecular anions, where interactions between sites can be approximately neglected. Thus the orbital and spin-dependent quantum mechanical energy spectrum of a single effective C_{60}^{3-} ion, once duly immersed in a crystal field of appropriate strength and cubic T_d symmetry, as sketched in Fig. 1, should provide a good representation for the MMI state and its excitation spectrum above T_N. With three electrons in three t_{1u} (p-like) orbitals, the effective ion site multiplet consists of, at frozen nuclei, three electronic terms, a high spin quartet ^4A ($L=0$, $S=3/2$), and two low spin doublets ^2H ($L=2$, $S=1/2$) and ^2T ($L=1$, $S=1/2$). On account of Hund's first rule, which dictates an energy $-J_H[2S(S+1) + L(L+1)/2]$,[24] the spin 3/2 term at $E = -(15/2)J_H$ should at frozen nuclei be the ground state, lying lower than the two spin 1/2 states, $E = -(9/2)J_H$, $E = -(5/2)J_H$ respectively.[26] However, as was anticipated, the intra-molecular exchange $J_H \sim 50\,meV$[24] is small, comparable with vibrational energies (30–150 meV) invalidating the frozen nuclei approximation, and causing a dynamical Jahn-Teller entanglement with vibrational states. That leads to a drastic reversal of these three states, now endowed with joint electron-nuclear character. Despite existing treatments[18–20,27,28] neither the specific role of orbital degrees of freedom nor the spectroscopic consequences of this entanglement appear to have been adequately addressed so far. The IR spectra in particular require specific first principles based calculations for each dynamical multiplet term characterising the Mott insulator, an agenda not implemented until now, but indispensable here as well as in future applications. The MMI spectrum is
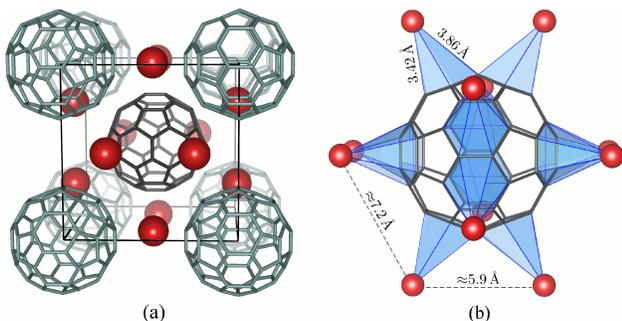
calculated as that of an uncoupled ion in the nanoscale crystal field model as on Fig. 1 (parameters given in Methods), in four steps. First, treating carbon nuclear coordinates as static variables, state-of-the-art density functional theory (DFT) electronic structure and molecular vibration calculations are carried out yielding the total energy, the optimal distortion away from T_d, and the full vibrational spectrum of the three statically distorted adiabatic states of spin 3/2 and 1/2 α, β, γ realized by three electrons in the initially t_{1u} molecular orbital. Second, for each of these adiabatic and distorted states the IR absorption spectra are calculated, again by accurate DFT methods. Third, the carbon nuclei in these statically distorted but unphysical states are allowed to delocalize by weak tunneling so as to give rise to three fully T_d-symmetric dynamical joint multiplet terms ^4A, ^2H, and ^2T of electrons and ions, with different energies from the static DFT states. Fourth and final, results for the IR absorption spectra corresponding to each multiplet state are derived from the previously calculated adiabatic spectra. Comparison with experiments clarifies the significance of IR peaks and splittings, whereas the overall temperature dependence reveals the thermal population of an important low lying orbital excitation.

II. METHODS

Near the C_{60}^{3-} ion the crystal field is mimicked by 12 point charges $q=0.25\,|e|$ at the Cs nuclear positions in Ganin et al.,[8] a setup which also averts self-ionization, yielding a ionization energy of approximately 2 eV similar to that of metallic fullerides. Spin polarized DFT calculations are carried out with the NWCHEM code. The B3LYP hybrid functional[29] polarization (DZVP) basis-set of 15 contracted functions, providing excellent DFT treatments of carbon – especially of exchange, here of vital importance. Accurate relaxation of C-atom positions and total energy minimization at $T=0$ gave rise to distortions, large in state γ, nil in α and small but nonzero in β, owing to a residual but real energy gain caused by splitting majority from minority spin levels. *Ab-initio* calculation of the 174 vibrational frequencies ω_i is carried out for fully relaxed states α, β, and γ and the resulting zero-point energies E_α, E_β, E_γ given in the text. The IR absorption spectra of states α, β, γ are calculated by evaluating dipole moments by numerical differentiation of the gradient at the equilibrium geometries, as implemented in NWCHEM.[30]

III. RESULTS AND DISCUSSION

A. Adiabatic states

We find by state-of-the-art DFT calculations (details given in Methods) the lowest energy electronic structure and static nuclear coordinates of C_{60}^{3-} in the cubic

FIG. 1. (a) Crystal structure of A15–Cs_3C_{60}.[9] (b) Assumed C_{60}^{3-} ion geometry. The crystal field is mimicked by 12 point charges $q=0.25\,|e|$ at the Cs nuclear positions in Ganin et al.[8]

environment of Fig. 1 for three different configurations, obtained by the following occupancies of three orbitals denoted as (x,y,z): $|\alpha\rangle$: occupancies $n_{x\uparrow}=1$, $n_{y\uparrow}=1$, $n_{z\uparrow}=1$, optimal nuclear symmetry T_d $S_z=3/2$; $|\beta\rangle$: occupancies $n_{x\uparrow}=1$, $n_{y\downarrow}=1$, $n_{z\uparrow}=1$, optimal nuclear symmetry D_{5d}, $S_z=1/2$; $|\gamma\rangle$: occupancies $n_{x\uparrow}=n_{x\downarrow}=1$, $n_{z\uparrow}=1$, optimal nuclear symmetry D_{2h}, $S_z=1/2$. Structurally, state $|\alpha\rangle$ is undistorted, 24 of its carbon atoms at a distance from the center $d=d_0=12.7175$, 24 at 12.7095 A, 12 at 12.6997 A. State $|\gamma\rangle$ is on the contrary heavily Jahn-Teller D_{2h} distorted, with $\sqrt{(1-d/d_0)^2}\sim 10^{-2}$. State $|\beta\rangle$ finally, exhibits a very small D_{5d} distortion, entirely due to electron-electron interactions, with $\sqrt{(1-d/d_0)^2}\sim 10^{-4}$. For each optimal state $|\alpha\rangle$, $|\beta\rangle$,$|\gamma\rangle$ we then calculate the full vibrational spectrum and from that the respective zero-point energy correction, ending up with the following total energy sequence: $E_\alpha-E_\gamma=66.0$ meV and $E_\beta-E_\gamma=27.1$ meV.

B. IR spectra of adiabatic states

In each adiabatic state $|\alpha\rangle$, $|\beta\rangle$, $|\gamma\rangle$ we calculate, as detailed in Methods, the *ab-initio* IR absorption spectra I_α, I_β and I_γ shown in Fig. 2 in comparison with the IR spectrum calculated for neutral C_{60} in same geometry (panel (a)).

Neutral C_{60} possesses four IR active $T_{1u}(n)$ modes, $n=1,...4$. In the crystal-field caged ion, IR peaks are red shifted relative to their neutral counterparts – especially $T_{1u}(4)$. Moreover, the $T_{1u}(1)$ peak amplitude near $520\,\text{cm}^{-1}$ vanishes in the ion while the $T_{1u}(3)$ peak at about $1200\,\text{cm}^{-1}$ weakens. Two additional differences characterize the heavily distorted state $|\gamma\rangle$. First, the IR modes are split and modified due to nonlinearities caused by the nuclear distortion, each T_{1u} mode splitting into $B_u+A_u+B_u$. Second, other *ungerade* modes such as H_u and T_{2u}, IR silent in the neutral undistorted molecule, develop components with an electric dipole, IR active in this state. Conversely, in state β (negligibly small distortion) and in α (zero distortion) there are no visible mode splittings and no new lines, so the IR spectrum is much simpler and closer to neutral C_{60}. These calculated spectra are not final however, the calculations requiring quantum delocalization of nuclei before experimental comparison, as explained below.

C. Fully symmetric multiplet states

The adiabatic states $|\alpha\rangle$, $|\beta\rangle$, $|\gamma\rangle$ do not correctly describe MMI multiplets , because by construction they artificially break both spatial and spin rotational invariance—they generally are symmetry-broken, as well as spin contaminated. The real dynamical MMI state must have fully orbital and spin rotational symmetry, namely ^2T, ^4A and ^2H now again within T_d ion, but with different IR properties, which we presently calculate.
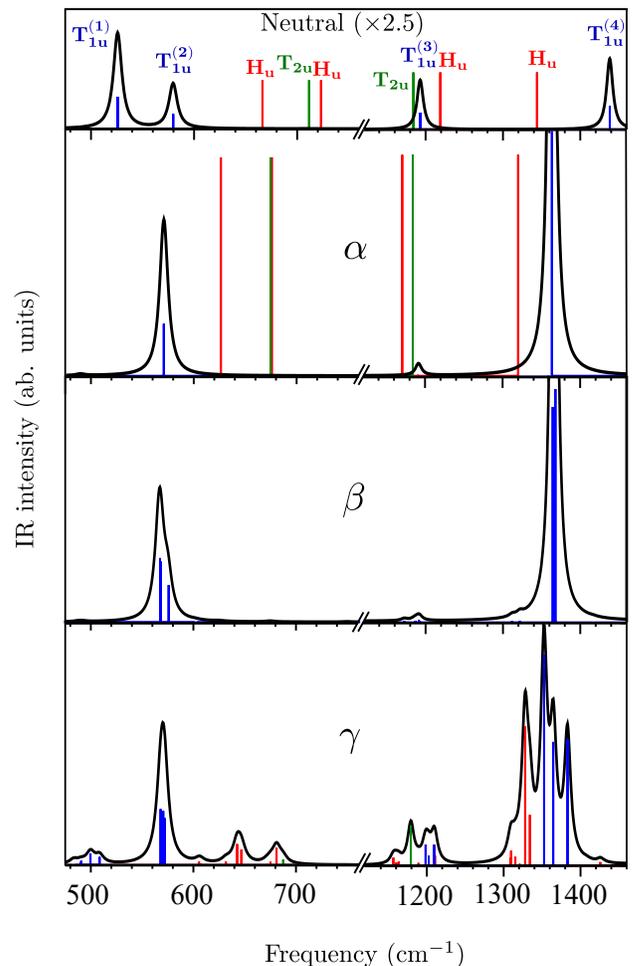

FIG. 2. (a)–(d): Calculated IR spectra of neutral C_{60} and of C_{60}^{3-} in DFT statically optimized states α, β and γ. The neutral case scale is multiplied by 6. Red and green lines indicate optically forbidden modes, becoming partly allowed in heavily distorted state γ.

Consider for instance $S_z=1/2$ state $|\gamma\rangle=c_{z\uparrow}^\dagger c_{x\uparrow}^\dagger c_{x\downarrow}^\dagger|0\rangle\times|\Phi\rangle$. The vibrational wavefunction Φ can be written as $\Phi=\Phi_e+\Phi_o$, the sum of two components that differ by parity, even (e) or odd (o), of the number of vibrational modes of the undistorted C_{60}^{3-}. The approximate expression of the rotationally symmetric doublet state ^2T is

$$|^2T\rangle \sim c_{z\sigma}^\dagger\left(c_{x\uparrow}^\dagger c_{x\downarrow}^\dagger+c_{y\uparrow}^\dagger c_{y\downarrow}^\dagger\right)|\Phi_e\rangle$$
$$+c_{z\sigma}^\dagger\left(c_{x\uparrow}^\dagger c_{x\downarrow}^\dagger-c_{y\uparrow}^\dagger c_{y\downarrow}^\dagger\right)|\Phi_o\rangle, \quad (1)$$

Its orthogonal doublet partner is instead

$$|^2H\rangle \sim c_{z\sigma}^\dagger\left(c_{x\uparrow}^\dagger c_{x\downarrow}^\dagger+c_{y\uparrow}^\dagger c_{y\downarrow}^\dagger\right)|\Phi_o\rangle$$
$$+c_{z\sigma}^\dagger\left(c_{x\uparrow}^\dagger c_{x\downarrow}^\dagger-c_{y\uparrow}^\dagger c_{y\downarrow}^\dagger\right)|\Phi_e\rangle, \quad (2)$$

It thus follows that

$$|\gamma\rangle \sim \sqrt{\frac{1}{2}}\left[|^2T\rangle+|^2H\rangle\right]. \quad (3)$$

By a similar argument we infer that

$$|\beta\rangle = c_{x\uparrow}^\dagger c_{y\downarrow}^\dagger c_{z\uparrow}^\dagger |0\rangle \times |\Phi'\rangle \sim \sqrt{\frac{1}{3}}\,|^4A\rangle + \sqrt{\frac{2}{3}}\,|^2H\rangle, \quad (4)$$

while $|\alpha\rangle = |^4A\rangle$. Direct support to Eqs. (3) and (4) comes from calculating by DFT the total spin expectation values, which we find to be $<\alpha|S^2|\alpha> \simeq 15/4$, $<\gamma|S^2|\gamma> \simeq 3/4$, and $<\beta|S^2|\beta> = 1.77 \simeq 7/4$ exactly as predicted by these equations. Inverting the transformation,

$$\begin{aligned}
E_{^4A} &= E_\alpha, \\
E_{^2H} &= \frac{3}{2}E_\beta - \frac{1}{2}E_\alpha, \quad (5)\\
E_{^2T} &= 2E_\gamma - \frac{3}{2}E_\beta + \frac{1}{2}E_\alpha,
\end{aligned}$$

where $E_{^4A} = E_\alpha$ is now set conventionally to zero. Inserting the calculated values of E_γ and E_β we obtain the final multiplet energies, namely $E_{^2H} = -58.3$ meV, $E_{^2T} = -73.7$ meV $E_{^4A} = 0$. The 1.6 μ_B moment observed by NMR in A15 Cs_3C_{60} above T_N agrees well with 1.73 of our ^2T ground state.[16] A spin excitation gap of order 800 K well established here as in other fullerides[16,31] is in agreement with the large $^4A -^2T$ calculated gap.

Now, as anticipated, the ^2H state is found a mere $\sim 15 \pm 6$ meV above the ^2T ground state. Unlike the $^2T \rightarrow^4 A$ spin-flip excitation, the excitation $^2T \rightarrow^2 H$, as could have been perhaps argued from previous theory work[19,23,24,28,32,33] takes place between spin doublets, and is thus of strictly orbital character ($L = 1 \rightarrow L = 2$). It is analogous in this respect to the "$d - d$" "orbitons" theorized[34,35] and observed[3] at much higher energy in transition metal based Mott insulators. In Cs_3C_{60} the large ion size and the consequently small exchange J_H lowers this excitation down into the range of nuclear vibrations and dynamical Jahn-Teller terms, with which it becomes entangled by hybridization. Optically forbidden by parity, this orbital excitation is low enough in energy to become thermally populated even below room temperature.

D. Temperature dependent IR Spectrum

Our first principles approach yields quantitative predictions for the infrared spectra of the Mott state, in any of its multiplet states. Each state has a different IR spectrum, directly obtainable from that, DFT-calculated, of the three adiabatic states. First, $I_{^4A} = I_\alpha$, because the two states are identical. Second, from Eq. (4) we obtain that $2I_{^2H} \simeq 3I_\beta - I_\alpha \simeq 2I_\beta$. The IR spectrum of the ground state ^2T finally, not calculable exactly through Eq. (3) owing to the unknown interference with ^2H in I_γ, is reasonably approximated by $I_{^2T} \simeq I_\gamma$, We finally compare in Fig. 3 these theoretical predictions with the experimental IR spectra,
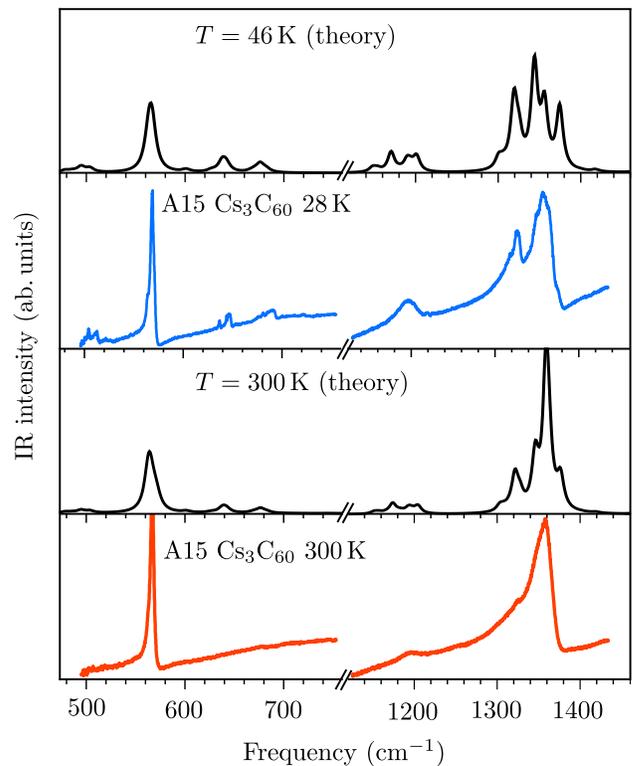

FIG. 3. IR spectra of Mott insulating Cs_3C_{60} (A15) (from Ref.[36]) compared with calculated ones $I(\omega,T) = \Sigma_{i=^2T,^2H,^4A} I_i(\omega)exp-E_i/k_BT$ at and above $T_N \sim 46\,K$, displayed with an arbitrary but reasonable broadening width $\sim 10cm^-1$ The thermal attenuation of all $T_{1u}(4)$ splittings and of other distortion-related peaks characteristic of the ^2T ground state is caused by population of the orbital excitation ^2H rather than to simple washing out of all distortions

both at low temperature and in their temperature evolution. Well below room temperature the spectrum is dominated by the ground state ^2T whose IR is similar to I_γ, sporting heavy traces of nuclear distortions.[12,36,37] The main peak near 1370 cm^{-1}, attributed to $T_{1u}(4)$, is split in three components, two of which are visible in experiment (a third one is actually visible in the fcc structure).[36,37] Importantly, new peaks near 640, 680, 1200, 1330 cm^{-1} are prominent in our calculation, in good correspondence with experiment at 28 K They are caused by B_u modes originating from H_u and some T_{2u} ones, formerly silent but now partly allowed by the large size ground state nuclear distotion.

Around room temperature instead we expect the total thermal population of the tenfold degenerate ^2H orbital excitation to become comparable with that of the sixfold-degenerate ^2T ground state. Consequently the IR spectrum is increasingly dominated by $I_{^2H} \simeq I_\beta$, causing the resulting intensity demise of splittings and new peaks, that are distortion-related features. This temperature-induced demise, previously attributed to the thermal washing out the classica adiabatic distortions (not unreasonably, but in reality puzzlingly at the

quantum level because of the much larger stabiliztion energies signaled by the $\sim 800\,\mathrm{K}$ $^2T \to {}^4A$ excitation across the spin gap) in fact represents the signature of the $^2T \to {}^2H$ orbital excitation. Were it not for the low-lying ^2H orbital excitation, the nuclear distortions, surely still strong at room temperature, would not permit the IR extra peaks and splittings to either attenuate or disappear. The thermal frailty of these distortion-related IR features represents the "smoking gun" of orbital excitations in the molecular Mott insulator.

Before closing we should mention that additional physical phenomena to those described so far will occur below the Néel temperature, $T_N \sim 46\,K$. In this regime the symmetry-breaking onset of antiferromagnetism introduces a Kugel-Khomskii coupling between spin and orbital degrees of freedom.[24] Consequences will include the onset of a static orbital distortion, and a corresponding magnon-orbiton coupling. The IR spectra and their description will also undergo weak modifications, expected to be weak but probably not undetectable experimentally. These aspects are left for future work.

IV. CONCLUSIONS

In summary, we have carried out a first realization of a program, where low-lying multiplet states of molecular Mott insulating have been quantitatively derived,

and their signature characterized spectroscopically for the first time by nanoscale site calculations which respect the full orbital symmetry, generally violated by first-principles approaches. The lowest excited state, an important feature of the MMI so far neglected, with mixed electronic-nuclear character but purely orbital in character, has been addressed and shown to be responsible for the experimental washing out of most distortion related features observed in IR spectra at temperatures above ~ 200–$300\,K$ without a simultaneous diappearance of the overall dynamic distortion. A similar fate and role of an orbital excitation, which is low-lying in A15-Cs_3C_{60} because of the nanoscale as opposed to atomic size of the insulating site, could be pursued in other MMIs in the future. On the given system, on the other hand, other properties including EPR spectra would very likely be influenced by the dynamic orbital physics outlined here.

[1] J. B. Goodenough, J. Solid State Chem. **3**, 490 (1971).

[2] K. I. Kugel' and D. I. Khomski, Sov. Phys. Usp. **25**, 231 (1982).

[3] J. Schlappa, K. Wohlfeld, K. J. Zhou, M. Mourigal, M. W. Haverkort, V. N. Strocov, L. Hozoi, C. Monney, S. Nishimoto, S. Singh, A. Revcolevschi, J.-S. Caux, L. Patthey, H. M. Rønnow, J. van den Brink, and T. Schmitt, Nature **485**, 82 (2012).

[4] C. Castellani, C. R. Natoli, and J. Ranninger, Phys. Rev. B **18**, 4945 (1978).

[5] S. Ishihara, M. Yamanaka, and N. Nagaosa, Phys. Rev. B **56**, 686 (1997).

[6] J. van den Brink and D. Khomskii, Phys. Rev. B **63**, 140416 (2001).

[7] G. Khaliullin and S. Maekawa, Phys. Rev. Lett. **85**, 3950 (2000).

[8] A. Y. Ganin, Y. Takabayashi, Y. Z. Khimyak, S. Margadonna, A. Tamai, M. J. Rosseinsky, and K. Prassides, nature materials **7**, 367 (2008).

[9] Y. Takabayashi, A. Y. Ganin, P. Jeglič, D. Arčon, T. Takano, Y. Iwasa, Y. O. nad, M. Takata, N. Takeshita, K. Prassides, and M. J. Rosseinsky, Science **323**, 1585 (2009).

[10] Y. Ihara, H. Alloul, P. Wzietek, D. Pontiroli, M. Mazzani, and M. Riccò, Phys. Rev. Lett. **104**, 256402 (2010).

[11] A. Y. Ganin, Y. Takabayashi, P. Jeglič, D. Arčon, A. Potočnik, P. J. Baker, Y. Ohishi, M. T. McDonald, M. D. Tzirakis, A. McLennan, G. R. Darling, M. Takata, M. J. Rosseinsky, and K. Prassides, Nature **466**, 221 (2010).

[12] K. Kamarás and G. Klupp, Dalt. Trans. **43**, 7366 (2014).

[13] R. H. Zadik, Y. Takabayashi, G. Klupp, R. H. Colman, A. Y. Ganin, A. Potocnik, P. Jeglic, D. Arcon, P. Matus, K. Kamaras, Y. Kasahara, Y. Iwasa, A. N. Fitch, Y. Ohishi, G. Garbarino, K. Kato, M. J. Rosseinsky, and K. Prassides, Sci. Adv. **1**, e1500059 (2015).

[14] L. Baldassarre, A. Perucchi, M. Mitrano, D. Nicoletti, C. Marini, D. Pontiroli, M. Mazzani, M. Aramini, M. Riccó, G. Giovannetti, M. Capone, and S. Lupi, Sci. Rep. **5**, 15240 (2015).

[15] O. Gunnarsson, Rev. Mod. Phys. **69**, 575 (1997).

[16] P. Jeglič, D. Arčon, A. Potočnik, A. Y. Ganin, Y. Takabayashi, M. J. Rosseinsky, and K. Prassides, Phys. Rev. B **80**, 195424 (2009).

[17] P. Wzietek, T. Mito, H. Alloul, D. Pontiroli, M. Aramini, and M. Riccò, Phys. Rev. Lett. **112**, 066401 (2014).

[18] L. F. Chibotaru, Phys. Rev. Lett. **94**, 186405 (2005).

[19] N. Iwahara and L. F. Chibotaru, Phys. Rev. Lett. **111**, 056401 (2013).

[20] N. Iwahara and L. F. Chibotaru, Phys. Rev. B **91**, 035109 (2015).

[21] A. Georges, G. Kotliar, W. Krauth, and M. Rozenberg, Rev. Mod. Phys. **68**, 13 (1996).

[22] O. Gunnarsson, E. Koch, and R. M. Martin, Phys. Rev. B **54**, R11026 (1996).

[23] M. Capone, M. Fabrizio, C. Castellani, and E. Tosatti, Science **296**, 2364 (2002).

[24] M.Capone, M.Fabrizio, C.Castellani, and E.Tosatti, Rev. Mod. Phys. **81**, 943 (2009).

[25] Y. Nomura, S. Sakai, M. Capone, and R. Arita, J. Phys. Condens. Matter **28**, 153001 (2016).

[26] F. Negri, G. Orlandi, and F. Zerbetto, Chem. Phys. Lett. **189**, 495 (1992).

[27] A. Auerbach, N. Manini, and E. Tosatti, Phys. Rev. B **49**, 12998 (1994).

[28] M. C. M. O'Brien, Phys. Rev. B **53**, 3775 (1996).

[29] A. D. Becke, j. chem. phys. **98**, 5648 (1993).

[30] M. Valiev, E. Bylaska, N. Govind, K. Kowalski, T. Straatsma, H. van Dam, D. Wang, J. Nieplocha, E. Apra, T. Windus, and W. de Jong, Comput. Phys. Commun. **181**, 1477 (2010).

[31] V. Brouet, H. Alloul, T.-N. Le, S. Garaj, and L. Forró, Phys. Rev. Lett. **86**, 4680 (2001).

[32] N. Manini, E. Tosatti, and A. Auerbach, Phys. Rev. B **49**, 13008 (1994).

[33] M. Capone, M. Fabrizio, C. Castellani, and E. Tosatti, Phys. Rev. Lett. **93**, 047001 (2004).

[34] S. Ishihara, J. Inoue, and S. Maekawa, Phys. Rev. B **55**, 8280 (1997).

[35] J. van den Brink, W. Stekelenburg, D. I. Khomskii, G. A. Sawatzky, and K. I. Kugel, Phys. Rev. B **58**, 10276 (1998).

[36] G. Klupp, P. Matus, K. Kamarás, A. Y. Ganin, A. McLennan, M. J. Rosseinsky, Y. Takabayashi, M. T. McDonald, and K. Prassides, Nature Communications **3**, 912 (2012).

[37] K. Kamarás, G. Klupp, P. Matus, A. Y. Ganin, A. McLennan, M. J. Rosseinsky, Y. Takabayashi, M. T. McDonald, and K. Prassides, J. Phys.: Conf. Ser. **428**, 012002 (2013).